Received: 29 January 2020 | Revised: 14 June 2020 | Accepted: 23 June 2020

DOI: 10.1111/cas.14549

Cancer Science WILEY

ORIGINAL ARTICLE

Novel cucurmosin-based immunotoxin targeting programmed cell death 1-ligand 1 with high potency against human tumor in vitro and in vivo

Caiyun Zhang[1] | Jiani Xiong[1,2] | Yinxiang Lan[1] | Jingyu Wu[1] | Chengyan Wang[3] | Zhihong Huang[4] | Jizhen Lin[5] | Jieming Xie[1]

[1]Department of Pharmacology, School of Pharmacy, Fujian Provincial Key Laboratory of Natural Medicine Pharmacology, Fujian Medical University, Fuzhou, China

[2]Department of Medical Oncology, Fujian Provincial Cancer Hospital, Fujian Medical University Cancer Hospital, Fuzhou, China

[3]Institute of Laboratory Animal Center, Fujian Medical University, Fuzhou, China

[4]Public Technology Service Center, Fujian Meidcal University, Fuzhou, China

[5]The Cancer Center, Union Hospital, Fujian Medical University, Fuzhou, China

***Correspondence**
Jieming Xie, Department of Pharmacology, School of Pharmacy, Fujian Medical University, Fuzhou, China.
Email: jmxie@fjmu.edu.cn

Jizhen Lin, The Cancer Center, Union Hospital, Fujian Medical University, Fuzhou, China.
Email: linjizhen@fjmu.edu.cn

Funding information
National Natural Science Foundation of China, Grant/Award Number: 30772587; Natural Science Foundation of Fujian Province, Grant/Award Number: 2016J01769; Fujian province health and family planning scientific research talent training project, Grant/Award Number: 2018-CX-40; Startup Fund for scientific research, Fujian Medical University, Grant/Award Number: 2019QH1196

Abstract

Immunotoxins are Ab-cytotoxin chimeric molecules with mighty cytotoxicity. Programmed cell death 1-ligand 1 (PD-L1), is a transmembrane protein expressed mainly in inflammatory tumor tissues and plays a pivotal role in immune escape and tumor progression. Although PD-L1 immune checkpoint therapy has been successful in some cases, many patients have not benefited enough due to primary/secondary resistance. In order to optimize the therapeutic efficacy of anti-PD-L1 mAb, we used durvalumab as the payload and CUS_{245C}, a type I ribosome-inactivating protein isolated from *Cucurbita moschata*, as the toxin moiety, to construct PD-L1-specific immunotoxin (named D-CUS_{245C}) through the engineered cysteine residue. In vitro, D-CUS_{245C} selectively killed PD-$L1^+$ tumor cells. In vivo studies also showed that D-CUS_{245C} had obvious antitumor effect on PD-$L1^+$ human xenograft tumors in nude mice. In conclusion, in the combination of the toxin with mAb, this study developed a new immunotoxin targeting PD-L1, emphasizing a novel and promising treatment strategy and providing a valuable way to optimize cancer immunotherapy.

KEYWORDS

cucurmosin, durvalumab, immunotoxin, PD-L1, targeted therapy

Caiyun Zhang and Jiani Xiong contributed equally to this work.

1 | INTRODUCTION

Antibody-based biological drugs are one of the well-accepted therapeutic strategies in cancer therapy.[1,2] Immunotoxins (ITs) are Ab-cytotoxin chimeric molecules with specific cell killing ability.[3] Immunotoxins are designed to kill tumor cells by attaching toxins to mAbs. The toxins used to make ITs are usually originated from plant (eg ricin, gelonin, and saporin), or bacteria (eg diphtheria toxin and *Pseudomonas* exotoxin A). Due to their high cytotoxicity, specificity, and effectivity, ITs show great antitumor potential in cancer immunotherapy.[4–8]

Programmed cell death 1-ligand 1 (PD-L1), also known as B7-H1 or CD274, is a type I transmembrane glycoprotein. When it binds to programmed cell death protein 1 (PD-1), it can inhibit activated T cell proliferation and biofunctions.[9] Accumulating evidence has shown that interactions between PD-1 and PD-L1 can lead to T cell anergy, exhaustion, and apoptosis, thereby inhibiting T cell-mediated cell killing, allowing tumors to evade immune surveillance.[10,11] Although various PD-L1 inhibitors have been developed for clinical treatment to release long-term antitumor responses in different cancer treatments,[12,13] many patients fail to respond due to primary resistance; others who have shown encouraging initial responses to immunotherapy might acquire resistance over time. By using a toxin conjugated to a PD-L1 Ab, to some extent, the limitations of checkpoint inhibition can be overcome, which is likely to determine the optimal use and efficacy of immunotherapy.

Cucurmosin (CUS) is a typical type I ribosome-inactivating protein (RIP)[14] isolated from *Cucurbita moschata* by our group. We determined the DNA sequence and the spatial structure of it[15] and examined the cytotoxicity compared to luffaculin and trichosanthin. In the past few years, our laboratory has been committed to the development of CUS-based ITs.[16,17] To facilitate production and cross-linking with other Abs, a cysteine residue was inserted at the 245th amino acid sequence of recombinant CUS to form a disulfide bond utilizing gene engineering.

Durvalumab, an intact humanized IgG1 mAb targeting PD-L1, it was approved by FDA for the treatment of stage III non-small-cell lung cancer after first-line treatment.[18,19] In this study, we used durvalumab as a payload and CUS_{245C} as a toxic agent to construct PD-L1-specific IT (named D-CUS_{245C}). In vitro results show that D-CUS_{245C} selectively kills cells that either stably expressed PD-L1 through plasmid transfection or inducibly expressed PD-L1 through γ-interferon-dependent signals, and showed antitumor activity of human cancers grown in immunodeficiency (nude) mice expressing PD-L1 antigen.

2 | MATERIALS AND METHODS

2.1 | Cell line

PD-L1/SPC-A-1 is a human lung carcinoma transfected stably with a PD-L1 cDNA, and the parental cell, NC/SPC-A-1 was used as a negative control. The human breast cancer cell line, MDA-MB-231, was purchased from the ATCC. All cells were cultured in RPMI-1640 medium (Gibco) supplemented with 10% FBS (Gibco).

2.2 | Reagent

Durvalumab (Imfinzi; AstraZeneca) was obtained from Universal Oncology Center. The FITC-anti-human PD-L1 (ab224074; Abcam), goat polyclonal Ab to human IgG (FITC) (ab81051; Abcam), Rb polyclonal Ab to 6× His-tag (FITC) (ab1206; Abcam), mouse-IgG_K BP-HRP (sc-516102; Santa Cruz Biotechnology). N-succinimidyl 3-(2-pyridyldithio)propionate (SPDP, 21857; Thermo Fisher Scientific). Human PD-L1 SimpleStep ELISA Kit (ab214565; Abcam).

2.3 | Flow cytometry

The expression of PD-L1 on the cell surface of PD-L1/SPC-A-1, NC/SPC-A-1, and MDA-MB-231 cell lines and binding capability of D-CUS_{245C} were assessed by flow cytometry on a FACSCalibur (BD Biosciences). To evaluate cell surface PD-L1 expression, cells were stained with the FITC-anti-human PD-L1 Ab. For verifying D-CUS_{245C} binding ability, durvalumab and D-CUS_{245C} were incubated with abovementioned cell lines and detected by anti-human-IgG (FITC) and anti-6× His tag (FITC), respectively, as a secondary Ab. Each experiment was repeated in triplicate.

2.4 | Enzyme-linked immunosorbent assay

The Human PD-L1 SimpleStep ELISA Kit was applied to detect whether the cell culture supernatant contains soluble PD-L1. The detailed procedures were carried out according to the kit instructions. In brief, we collected the cell-free culture supernatants from PD-L1/SPC-A-1, NC/SPC-A-1, and MDA-MB-231 cells at 72 and 120 hours. We diluted the standard to a concentration of 1100, 550, 275, 137.5, 68.75, 34.37, and 17.18 pg/mL, and set up blank control wells, then added 50 μL of all samples or standard to appropriate wells. Antibody cocktail (50 μL) was added to each well. The plate was sealed and incubated for 1 hour at room temperature on a plate shaker set to 400 rpm. After each well was washed with 3 × 350 μL 1X Wash Buffer PT, 100 μL TMB Development Solution was added to each well and incubated for 10 minutes in the dark. The reaction was stopped with the addition of 2.5 mol/L H_2SO_4. Absorbance was read at 450 nm. All samples and standards were tested in triplicate.

2.5 | Cellular imaging with confocal microscopy

CUS_{245C} and durvalumab were labelled with FITC using a Fluoreporter FITC Protein Labeling Kit (Thermo Fisher Scientific). The detailed procedures were undertaken according to the kit instructions. PD-L1/

SPC-A-1 and NC/SPC-A-1 cells were seeded in glass bottom cell culture dishes at a density of 1×10^4 cells per well and allowed to attach overnight. Next day, cells were incubated with 5 ng/mL FITC-labelled CUS_{245C} and durvalumab for 1, 2, 6, 12, and 24 hours. The plates were washed 3 times with PBS and nuclei were stained with Hoechst stains. Images were obtained by confocal microscopy using the LSM 710 system (Carl Zeiss) with 63× water C-Apochromat objective.

2.6 | Synthesis and characterization of D-CUS_{245C}

The expression and purification of CUS_{245C} was described previously.[16] The synthesis of the IT began with reduction of CUS_{245C} dimers by 0.3 mol/L DTT (Beyotime), according to the previously published method.[16] Meanwhile, 25 μL of the 20 mmol/L SPDP (Thermo Fisher Scientific) solution was added to 2-5 mg durvalumab in 1.0 mL PBS-EDTA and the mixture was incubated for 30 minutes at room temperature. A desalting column was equilibrated with PBS-EDTA, and the SPDP-modified IgG was used to remove reaction byproducts and excessive nonreacted CUS_{245C} and SPDP reagent. CUS_{245C} (7.45 mg; ~5 moles CUS_{245C} per mole of durvalumab) was added to the durvalumab solution and the mixture was incubated at 23°C for 18 hours. The synthetic reaction was terminated by 0.1 mol/L iodoacetamide. After centrifugation and dialysis, Float-A-Lyzer G2 with the 100 kDa MWCO (Spectrum Laboratories) was utilized to get rid of the free CUS_{245C}; the synthetic product, D-CUS_{245C}, was collected and purified with a Ni-NTA column. Purified product was analyzed on 6% and 12% SDS-PAGE gels.

2.7 | In vitro cytotoxicity assay

The cytotoxicity of synthetic IT was assessed with inhibition of protein synthesis in a dose-dependent manner. The dose- and time-dependent cytotoxic activities of IT were measured by sulforhodamine B (SRB) assays as previously described.[16] Briefly, cells at 3×10^4/mL per well in logarithmic phase were seeded in 96-well plates and incubated overnight before they were treated with CUS_{245C}, durvalumab, D-CUS_{245C}, or D+CUS_{245C} for 72 or 120 hours. Colorimetry was undertaken at 515 nm with an Epoch Microplate Reader (BioTek Instruments). The cytotoxic activity was defined by IC_{50} values. Each experiment was repeated in triplicate.

2.8 | Apoptosis assay

The FITC-annexin V apoptosis kit (KGA106; KeyGEN BioTECH) was used to evaluate the apoptotic effects of D-CUS_{245C} on PD-L1/SPC-A-1 and NC/SPC-A-1 cells. In preparation for the apoptosis assay, cells with a density of 5×10^4/mL per well were seeded in 6-well plates for 24 hours. The cells were then treated with D-CUS_{245C} at concentrations of 0.5, 2.5, or 5 nmol/L for 72 hours, or kept untreated. After that, cells were collected, centrifuged, counted, resuspended in PBS, and analyzed with flow cytometry (BD Biosciences).

2.9 | Antitumor activity in vivo

Six- to 8-week-old male athymic nude mice (nu/nu genotype, BALB/c background) were purchased from Shanghai SLAC Laboratory Animal Co. and kept at the animal facility of Fujian Medical University (Fuzhou, China). All of the animal procedures were carried out according to approved protocols and in accordance with recommendations for the proper use and care of laboratory animals (protocol no. FJMU IACUC 2019-0082).

To determine the antitumor activity of D-CUS_{245C}, approximately 2×10^6 PD-L1/SPC-A1 cells were suspended in 0.1 mL PBS and injected s.c. into the right forelimb of nude mice (n = 6–8 per group) on day 0. Tumors (approximately 50 mm^3 in size) were developed in the tumor cell-injected animals by day 4 after implantation. Starting on day 4, animals were treated with D-CUS_{245C} diluted in 0.2 mL PBS by i.v. injection on days 4, 8, 12, and 16. Tumors were measured with a caliper every 2 or 3 days, and the volume of the tumor was calculated by using the following formula: tumor volume (mm^3) = length × $(width)^2 \times 0.5$. Tumors from mice in the aforementioned 5 groups were separated and weighed after all treatments and observations were finished.

2.10 | Statistical analysis

All statistical data were analyzed using Prism 6.0 (GraphPad). Experimental data are presented as mean ± SD. Groupwise comparisons of mean data were made by Student's *t* test. Probability (*P*) values less than .05 were considered significant.

3 | RESULTS

3.1 | Cell surface and cell culture supernatant of PD-L1expression

The PD-L1 expression at the cell surface was determined by flow cytometry. As shown in Figure 1A, the PD-L1 stably transfected human lung cancer cell line, PD-L1/SPC-A-1, reacted strongly with the PD-L1 Ab, whereas the nontransfected parental cell line, NC/SPC-A-1, was used as negative control. The triple-negative breast cancer (TNBC) cell line, MDA-MB-231, which constitutively expresses PD-L1, had a relatively high fluorescence intensity after incubation with the FITC-conjugated PD-L1 Ab when compared with the negative control NC/SPC-A-1.

A sandwich ELISA system was established for the quantitative determination of soluble PD-L1 (sPD-L1) in the cell culture supernatant. The standard line in Figure 1C indicates the good specificity and line reliability of the sPD-L1 ELISA method from 22 up to 1400 pg/mL. The R^2 value is greater than .999. Figure 1D shows that, compared with the NC/SPC-A-1 cell line, transfected cell line PD-L1/SPC-A-1 produced a mass of sPD-L1 in the supernatants at a concentration of 1.3 ng/mL for 72 hours and 1.4 ng/mL for 120 hours.

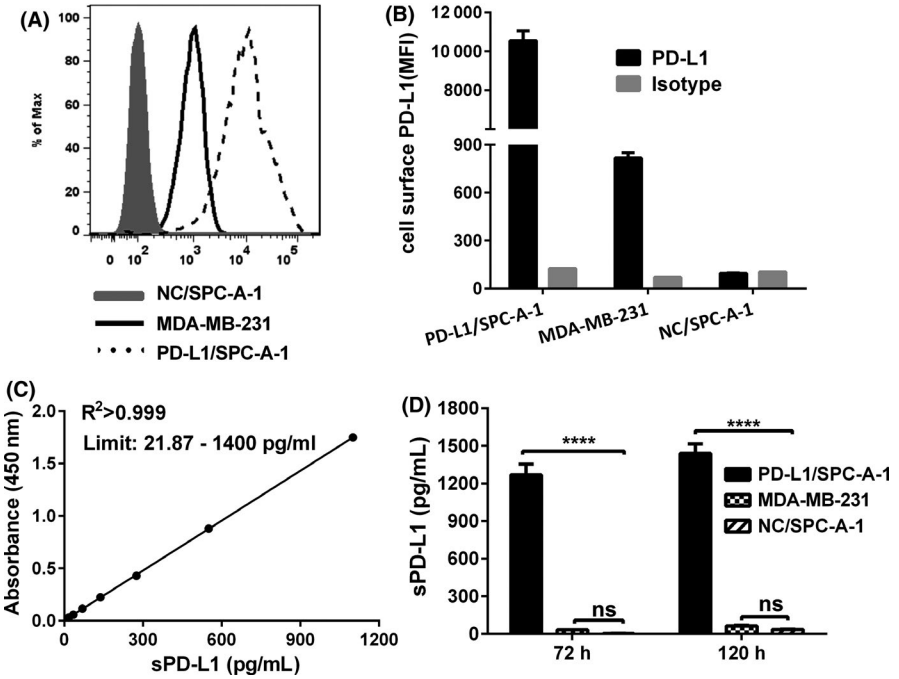

FIGURE 1 Detecting the expression of programmed cell death 1-ligand 1 (PD-L1). A, Flow cytometry determined the PD-L1 expression on the surface of various cells. B, Quantitative analysis of mean fluorescence intensity (MFI). A human soluble PD-L1 (sPD-L1) ELISA kit was used to determine PD-L1 in the cell culture supernatant. C, Correlation line of optical density at 450 nm absorbance and sPD-L1 concentration at determined detection limits. D, sPD-L1 levels in the supernatants of PD-L1/SPC-A-1, MDA-MB-231, and negative control (NC)/SPC-A-1 cells

Soluble protein levels detected in the supernatant of MDA-MB-231 cells were consistent with those of NC/SPC-A-1 cells ($P > .05$), indicating that PD-L1 protein was not released from the constitutively expressing PD-L1 cell membrane.

3.2 | Internalization of durvalumab in PD-L1$^+$ cells

Confocal microscopy indicated significant and specific internalization of durvalumab-FITC conjugate into the PD-L1/SPC-A-1 cells but not into NC/SPC-A-1 cells. Figure 2A shows that the fluorescence was observed on the cell surface when cells were incubated with durvalumab-FITC for 1 hour. At 2 hours, partial fluorescence was observed in the cytoplasm, but most of the fluorescence was still distributed on the membrane surface. The green fluorescence on the cell surface was weakened when the incubation time was extended to 6 hours, and granular blips with concentrated green fluorescence appeared in the cytoplasm. After 12 hours of incubation, the durvalumab- FITC conjugate was efficiently taken up by PD-L1/SPC-A-1 cells and localized in the cytoplasm. Durvalumab-FITC conjugate was barely detected in NC/SPC-A-1 cells when PD-L1 expression was absent (Figure 2B). Furthermore, the internalization of CUS_{245C}-FITC was also tested on the above 2 cell lines. After 24 hours of incubation, only faint fluorescence was detected in the cytoplasm (Figure 2C). These data indicate that CUS_{245C} barely entered into the cytoplasm without binding moiety.

3.3 | Synthesis and characterization of D-CUS_{245C}

To synthesize an IT targeting PD-L1, the recombinant CUS_{245C} was conjugated to the anti-PD-L1 mAb, durvalumab, through an artificial disulfide bond. Both 6% and 12% SDS-PAGE were used to analyze the molecular weight and purity of the conjugates we produced. As shown in Figure 3, the immunoconjugate (Figure 3A, lane 4) is a mixture with multiple molecular weight at 186, 214, and 242 kDa. Using dialysis and affinity chromatography, residual CUS_{245C} (Figure 3A, lane 6) and unconjugated durvalumab (Figure 3A, lane 5) were removed, respectively. The final product, named D-CUS_{245C}, is a mixture of PD-L1 Abs and CUS_{245C} at a ratio of 1:2, 1:3, or even 1:4. We then analyzed the gray values of CUS_{245C}, durvalumab, and D-CUS_{245C} with the reduced SDS-PAGE using ImageJ, and determined the ratio of heavy chain : light chain : CUS_{245C} as 2.54:1.00:1.32; therefore, the molecular weight of D-CUS_{245C} is approximately 230 kDa (durvalumab, 158 kDa).

Flow cytometry results (Figure 3C,D) showed that the conjugation procedures did not alter the mAb binding affinity. D-CUS_{245C} bound to the PD-L1$^+$ cells, PD-L1/SPC-A-1 and MDA-MB-231, and maintained the same affinity compared to durvalumab, but did not respond to PD-L1$^-$ cells, NC/SPC-A-1, indicating that IT D-CUS_{245C} retains the binding capability and binds to PD-L1.

3.4 | Cytotoxicity and apoptosis-inducing effects of D-CUS_{245C} on different cell lines

After conjugation, we used SRB assays to determine the cytotoxic activity of D-CUS_{245C} on 3 cancer cell lines. We exposed these cell lines to the CUS_{245C}, durvalumab, D-CUS_{245C}, and D+CUS_{245C} for 72 or 120 hours. Figure 4A shows dose-dependent cell killing of D-CUS_{245C} on PD-L1 overexpression cell lines, PD-L1/SPC-A-1 and MDA-MB-231, evaluated by SRB-based cytotoxicity assay. In the 72 hour/120 hour test, in the lung cancer cell line PD-L1/SPC-A-1, which reacted strongly with the PD-L1 Ab, the IC_{50} values of

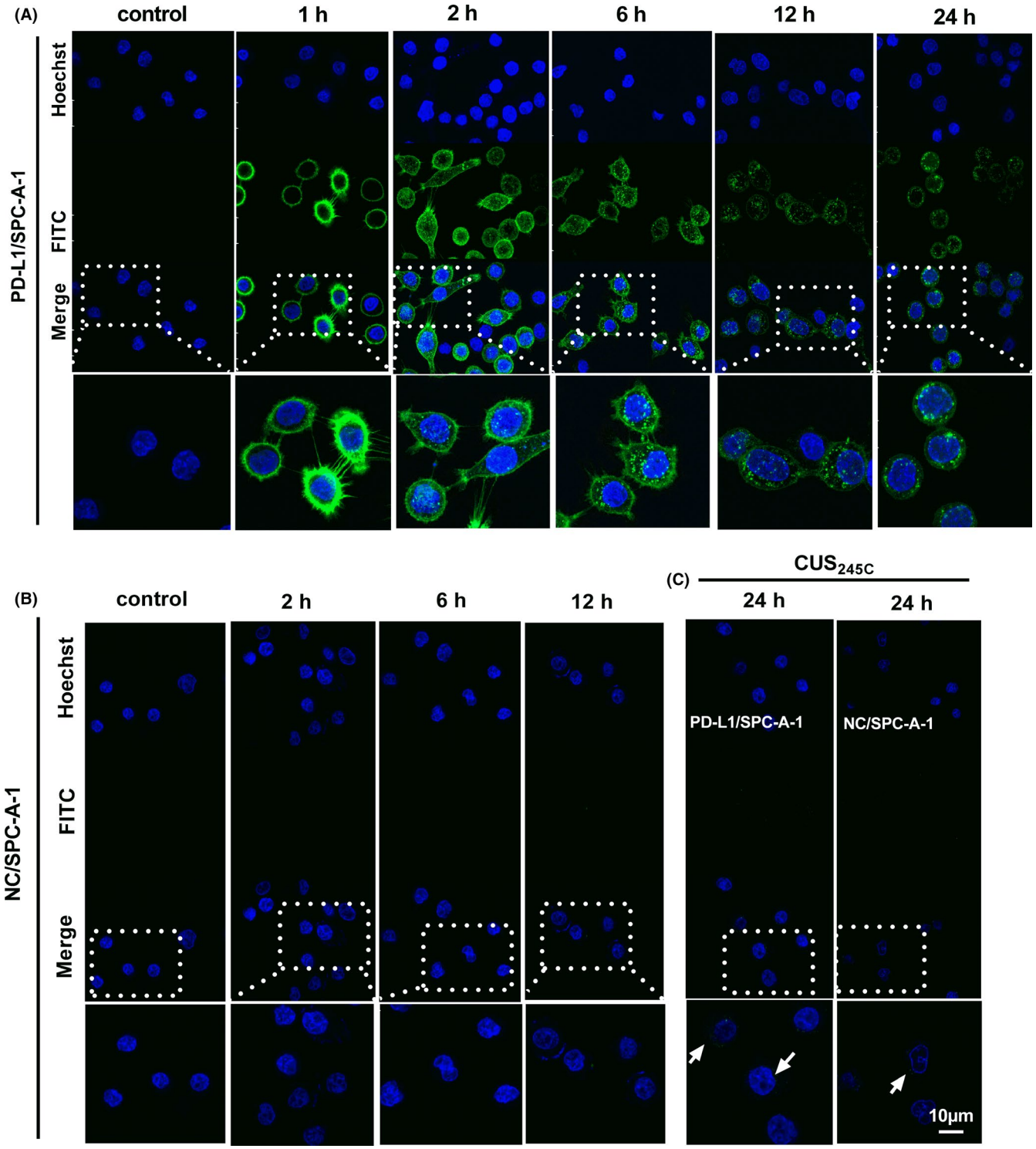

FIGURE 2 Programmed cell death 1-ligand 1 (PD-L1)-specific internalization of durvalumab confirmed by confocal microscopy. A, Internalized level of durvalumab at 1, 2, 6, 12, and 24 h in PD-L1/SPC-A-1 cells. B, Internalized level of durvalumab at 2, 6, and 12 h in negative control (NC)/SPC-A-1cells. C, PD-L1/SPC-A-1 and NC/SPC-A-1 cells treated with CUS_{245C} for 24 h. Cells were incubated with FITC-conjugated durvalumab (green). Nuclei were counterstained with Hoechst (blue). Scale bar = 10 μm

D-CUS_{245C} were 3.8 to 2.8 pmol/L, significantly higher than that of CUS_{245C} (363.3 nmol/L/365.7 nmol/L; $P < .0001$; Figure 4A, Table 1). The target index of D-CUS_{245C} to PD-L1/SPC-A-1 was approximately 140 000 at 120 hours.

The TNBC cell line MDA-MB-231 was more sensitive to D-CUS_{245C} with an IC_{50} of 1.6 pmol/L for 72 hours; in the 120 hour experiment, the IC_{50} values were 0.14 pmol/L, significantly lower than IC_{50} values of CUS_{245C} alone (503 and 154 nmol/L, respectively; $P < .0001$) (Figure 4A,

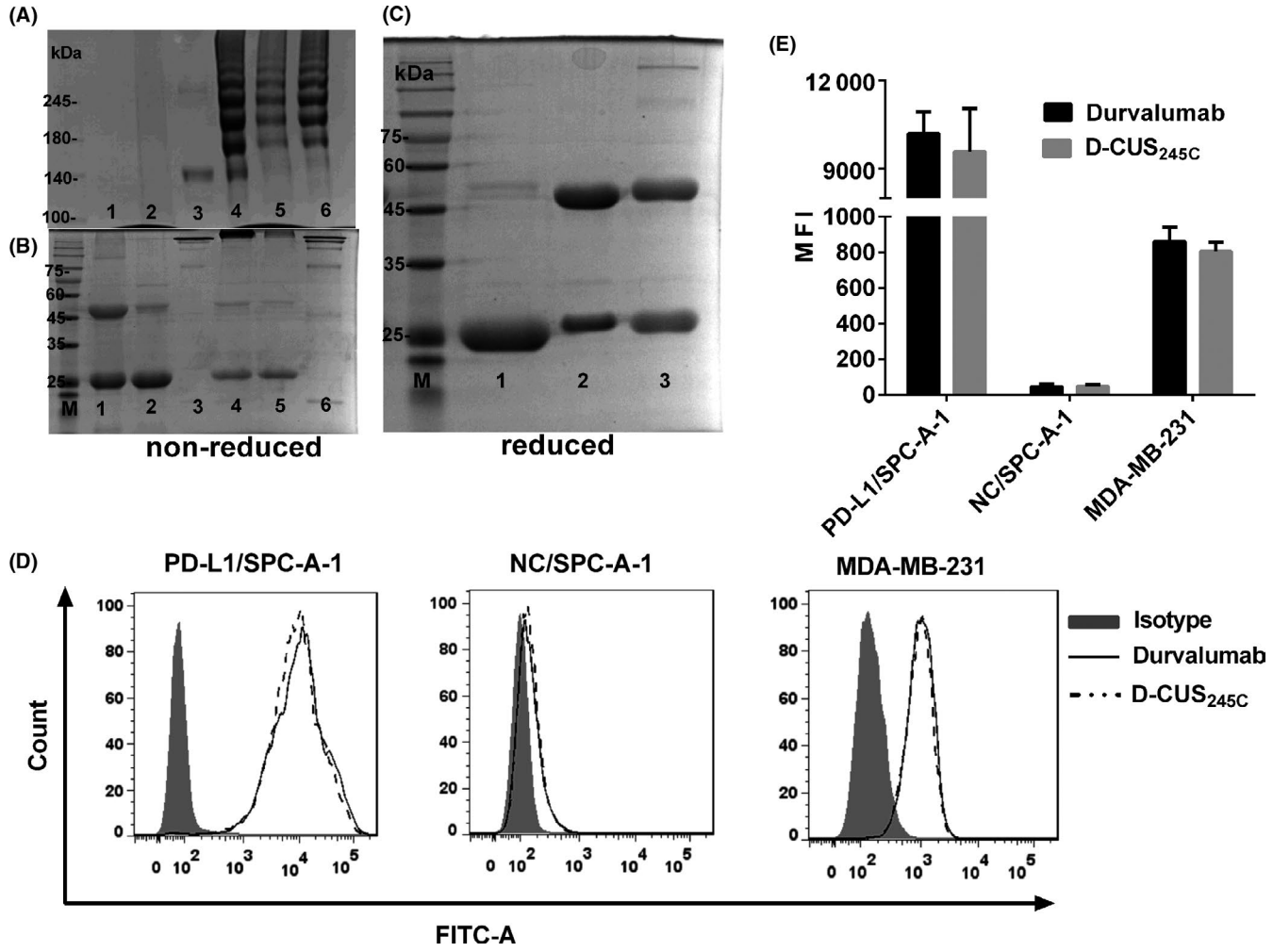

FIGURE 3 Generation, purification, and characterization of immunotoxin D-CUS_{245C}. A, B, 6% and 12% SDS-PAGE, respectively, under nonreduced conditions. Lane 1, dimers of CUS_{245C}; lane 2, monomers of CUS_{245C}; lane 3, durvalumab; lane 4, mixture from coupling; lane 5, coupling product purified by Ni-NTA column; lane 6, D-CUS_{245C}. C, SDS-PAGE under reduced conditions. Lane 1, CUS_{245C}; lane 2, durvalumab; lane 3, D-CUS_{245}. Standard molecular weights (M) are expressed in kDa. D, E, Affinity of D-CUS_{245C} compared with that of durvalumab by flow cytometry

Table 1), indicating a time-dependent cytotoxicity of both D-CUS_{245C} and $CUS_{245C.}$ The TI of the D-CUS_{245C} to MDA-MB-231 reached up to 300 000. It was not possible to calculate an IC_{50} value for free mAb or a mixture of unconjugated durvalumab and CUS_{245C} (D + CUS_{245C}).

Using NC/SPC-A-1 we investigated the specificity of the immunotoxins. Comparison with mAb or a mixture of unconjugated durvalumab and CUS_{245C}, the cytotoxicity of D-CUS_{245C} was not increased (Figure 4A, Table 1). At the maximum tested concentration (1 nmol/L), none of them reached the IC_{50} value at 72 or 120 hours.

Of interest, the level of the reaction of the cells to IT was independent of the level of expression of PD-L1. Both PD-L1/SPC-A-1 and MDA-MB-231 were PD-L1 overexpression cell lines, and PD-L1/SPC-A-1 has the highest PD-L1 expression level. NC/SPC-A-1 cells were considered as $PD\text{-}L1^{-}$ cells. In the cell killing assay, MDA-MB-231 was the most sensitive cell line to D-CUS_{245C}, while PD-L1/SPC-A-1 was relatively lower, suggesting that there are additional unknown mechanisms affect IT-induced cell death.

To determine the mechanism through which D-CUS_{245C} exerts its function of killing tumor cells, annexin V/phycoerythrin-based apoptosis assay was carried out to analyze the apoptosis of cells induced by these drugs. As shown in Figure 4B, D-CUS_{245C} caused little or no apoptosis on NC/SPC-A-1 cells at a variety of concentrations, indicating that D-CUS_{245C} did not induce apoptosis (less than 3%) on NC/SPC-A-1 cells which absence of PD-L1 expression. In contrast, the percentages of early and late apoptosis in D-CUS_{245C}-treated PD-L1/SPC-A-1 cells were significantly higher than that of

FIGURE 4 Cytotoxicity and apoptosis-inducing effects of immunotoxin D-CUS_{245C} on different cell lines. A, Cytotoxicity of CUS_{245C}, D-CUS_{245C}, durvalumab (D), and D + CUS_{245C} on different cells for 72 and 120 h by sulforhodamine B assay. B, Flow cytometry tested programmed cell death 1-ligand 1 (PD-L1)/SPC-A-1 and negative control (NC)/SPC-A-1 apoptosis induced by D-CUS_{245C} at different concentrations for 72 h. C, Percentages of dead cells, late apoptosis, early apoptosis, and live cells in PD-L1/SPC-A-1 and NC/SPC-A-1 cells treated with D-CUS_{245C} for 72 h. PI, propidium iodide

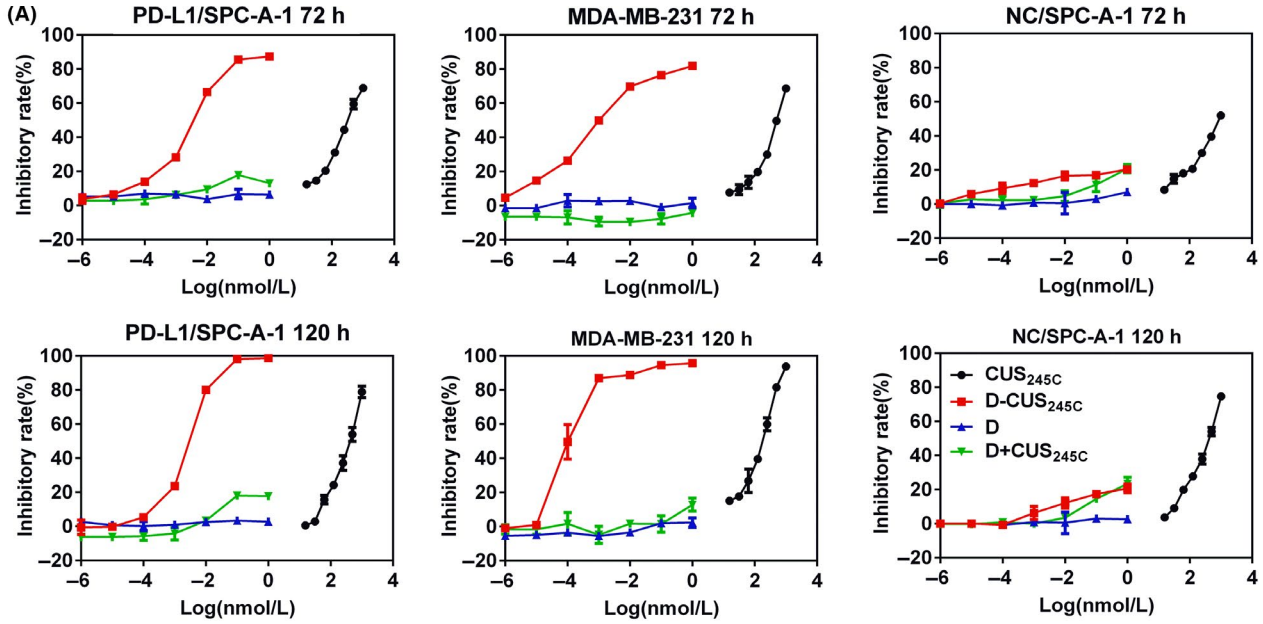
(A)
PD-L1/SPC-A-1 72 h
MDA-MB-231 72 h
NC/SPC-A-1 72 h
PD-L1/SPC-A-1 120 h
MDA-MB-231 120 h
NC/SPC-A-1 120 h
Inhibitory rate(%)
Log(nmol/L)
CUS245C
D-CUS245C
D
D+CUS245C

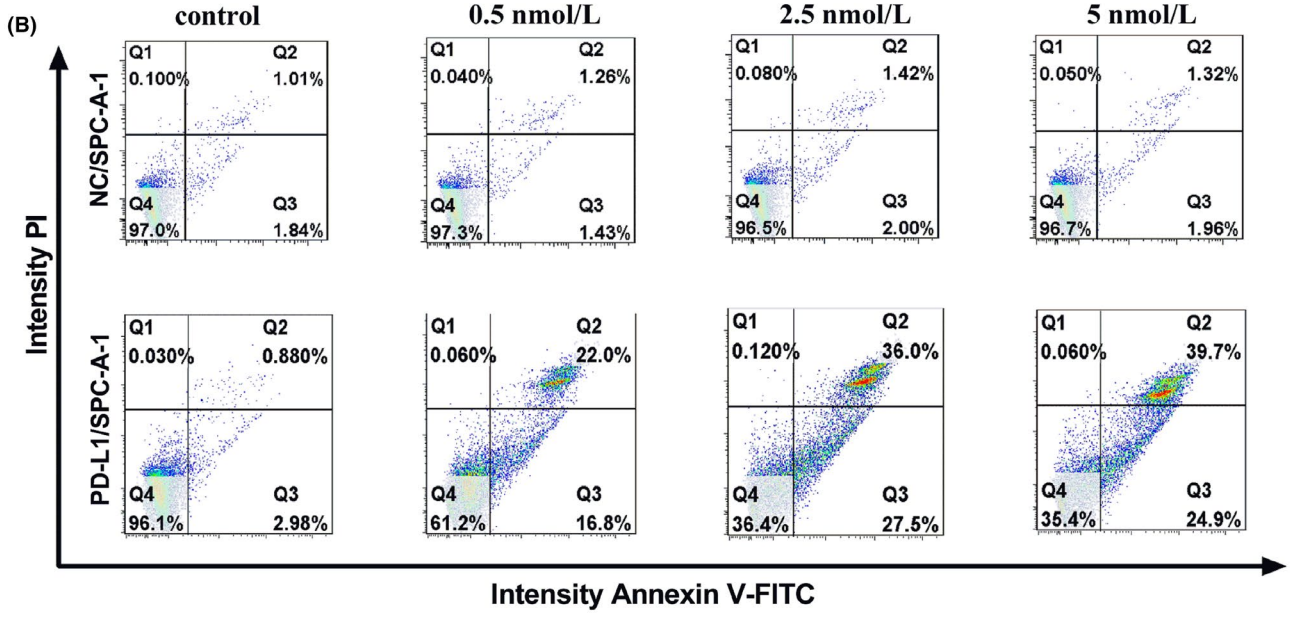
(B)
control
0.5 nmol/L
2.5 nmol/L
5 nmol/L
NC/SPC-A-1
PD-L1/SPC-A-1
Intensity PI
Intensity Annexin V-FITC
Q1 0.100% Q2 1.01% Q4 97.0% Q3 1.84%
Q1 0.040% Q2 1.26% Q4 97.3% Q3 1.43%
Q1 0.080% Q2 1.42% Q4 96.5% Q3 2.00%
Q1 0.050% Q2 1.32% Q4 96.7% Q3 1.96%
Q1 0.030% Q2 0.880% Q4 96.1% Q3 2.98%
Q1 0.060% Q2 22.0% Q4 61.2% Q3 16.8%
Q1 0.120% Q2 36.0% Q4 36.4% Q3 27.5%
Q1 0.060% Q2 39.7% Q4 35.4% Q3 24.9%

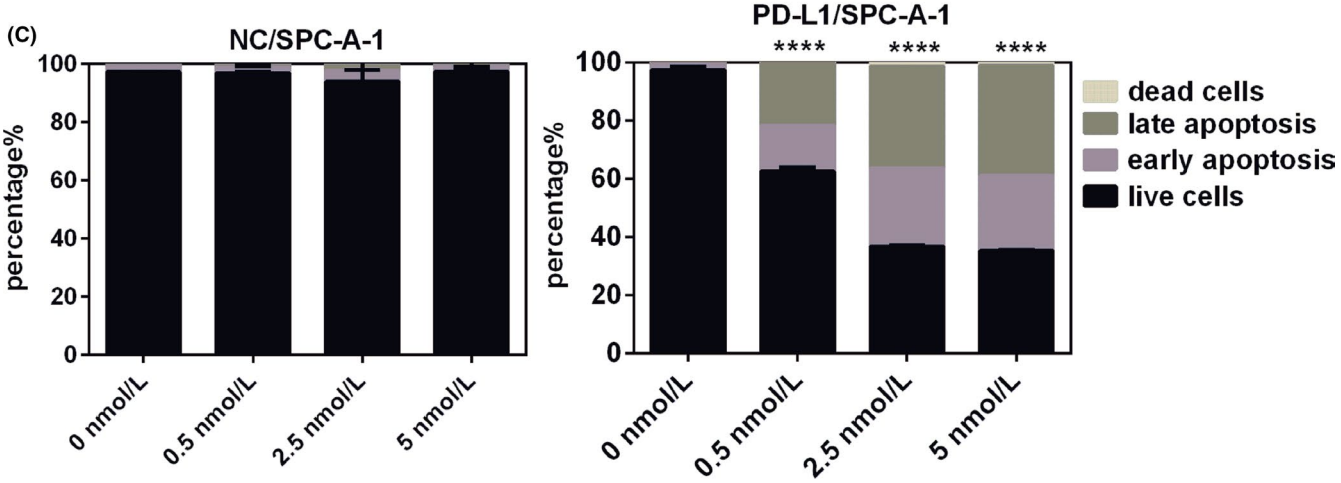
(C)
NC/SPC-A-1
PD-L1/SPC-A-1
percentage%
****
dead cells
late apoptosis
early apoptosis
live cells
0 nmol/L
0.5 nmol/L
2.5 nmol/L
5 nmol/L

TABLE 1 Inhibitory concentration (IC_{50}) values of cancer cells treated with drugs for 72 or 120 h

IC_{50} (mean ± SD)			
Cell line	**CUS_{245C} (nmol/L)**	**D-CUS_{245C} (pmol/L)**	**TI**
PD-L1/SPC-A-1 (72 h)	363.3 ± 10.68	3.8 ± 1.27****	88 026.3
PD-L1/SPC-A-1 (120 h)	365.7 ± 13.39	2.8 ± 0.081****	135 678.6
MDA-MB-231 (72 h)	503.7 ± 0.11	1.6 ± 0.11****	314 812.5
MDA-MB-231 (120 h)	154.3 ± 6.23	0.14 ± 0.0075****	1 102 143
NC/SPC-A-1 (72 h)	994.7 ± 33.63	›1000	—
NC/SPC-A-1 (120 h)	375.6 ± 13.56	›1000	—

****$P < .0001$, compared with CUS_{245C} (ribosome-inactivating protein isolated from *Cucurbita moschata*).

–, Cannot calculate within the concentration detection range; D-CUS_{245C}, immunotoxin conjugating by durvalumab and CUS_{245C}; TI, target index = $IC_{50}^{CUS_{245C}}/IC_{50}^{D\text{-}CUS_{245C}}$.

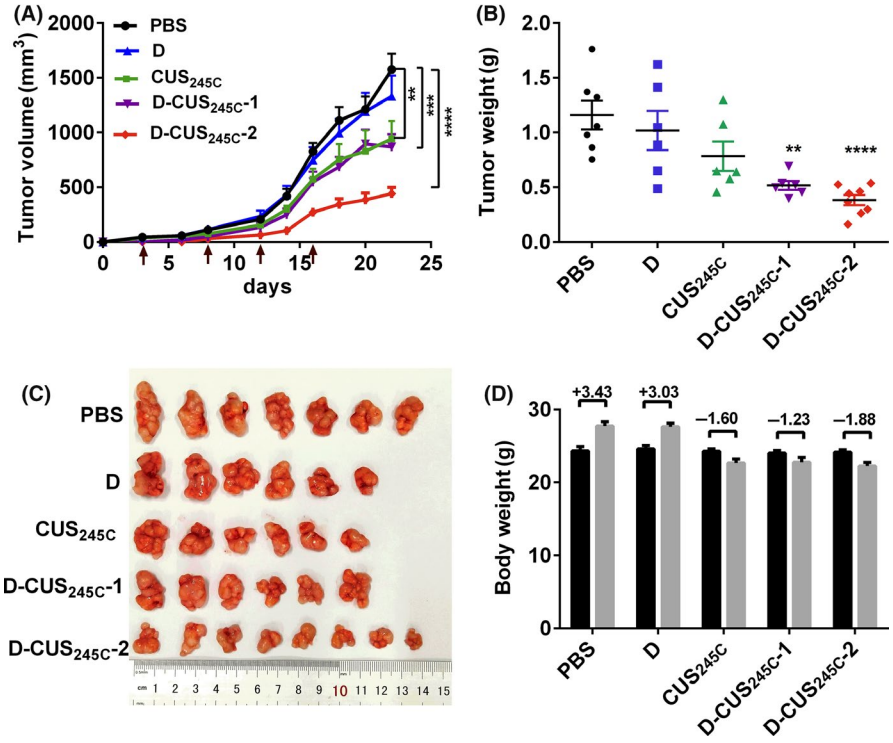

FIGURE 5 Antitumor activity of immunotoxin (IT) D-CUS_{245C} in nude mouse. A, Time course of tumor volume progression of programmed cell death 1-ligand 1 (PD-L1)/SPC-A-1-derived xenografts. Animals were nontreated (PBS) or treated i.v. on days 4, 8, 12, and 16 with 0.8 mg/kg durvalumab (D), 0.4 mg/kg CUS_{245C}, 0.4 mg/kg IT (D-CUS_{245C}-1), or 0.8 mg/kg IT (D-CUS_{245C}-2). B, Tumor weight. C, Tumor images. D, Body weight evolution in mice. Weight measurement before and after treatment. Black bars, before treatment; gray bars, 7 d after final treatment. Data are presented as mean ± SEM. **$P < .01$, ***$P < .001$, ****$P < .0001$ vs PBS

untreated control. The percentage of apoptosis was 38% at 0.5 nmol/L D-CUS_{245C}, and the apoptotic rate reached 65% as the concentration increased to 5 nmol/L, which was significantly different to the control group ($P < .0001$). These data showed that D-CUS_{245C} kills cells through the apoptosis pathway.

3.5 | Antitumor activity of D-CUS_{245C} in vivo

To determine the antitumor activity of D-CUS_{245C}, we treated nude mice harboring PD-L1/SPC-A-1 tumors with different doses of the IT, durvalumab, and CUS_{245C}. After tumors reached approximately 50 mm^3 4 days after implantation, the mice were randomized and then treated on days 4, 8, 12, and 16. Figure 5A shows that tumor regressions were observed in mice given 0.4 or 0.8 mg/kg D-CUS_{245C}. Compared to PBS-treated mice, both the tumor volume and mass decreased dramatically in the 2 IT dose groups (Figure 5A-C), with the higher dose producing a larger effect ($P < .0001$), suggesting that D-CUS_{245C} was able to suppress tumor growth (until the animals were killed). In mice subjected to the pressure of IT by study day 22, the mean tumor weight was reduced by 55% (D-CUS_{245C}-1) and 67% (D-CUS_{245C}-2) compared to the control groups treated with PBS. The average tumor volumes in the groups receiving 0.4 mg/kg CUS_{245C} were also significantly different ($P < .01$) from the average tumor volumes in the PBS-treated group but tumor weight was not statistically significant. No responses were noted with mice treated with 0.8 mg/kg durvalumab (Figure 5A-C).

Figure 5D shows that the body weight of mice decreased in all treatment groups (except the Ab group) after 2 weeks of treatment. However, the body weight index decrease did not exceed 20% compared with the previous treatment. During the experiment, none of

the animals died, and the animal body weight increased after 1 week of drug withdrawal (data not shown).

4 | DISCUSSION

It has been clear that the occurrence of many tumors is related to the immune escape mediated by the immune checkpoint PD-L1,[20] the blockade of the B7-H1 pathway has become a new strategy for the treatment of melanoma, lung, breast, and colon cancer.[12] Despite its impressive clinical success, only a small number of patients are likely to benefit from these therapies.[21] Immunotoxins are Ab-cytotoxin chimeric molecules that selectively and efficiently kill tumor cells by attaching the toxin to mAbs. By adding the toxin to the Ab, compared with the original PD-L1 inhibitors, the therapeutic efficacy can be enhanced multiple times. In this study, the toxin moiety we used (CUS) is a typical type I RIP, which can hydrolyze the A4324 N-glycosidic bond on the 28S rRNA of eukaryotic cells, irreversibly inactivating the ribosomal 60S subunit, and halts protein synthesis.[22,23] In most cases, as long as a toxin molecule enters the cell, it is enough to kill the cell. As the mechanism of action of ITs is to directly kill cells rather than inhibit receptor-mediated signaling pathways, tumor cells might be less likely to upregulate rescue mutations or substitute signaling pathways to resist IT therapy.

The mechanism of action of ITs includes the binding of its target region to the tumor-associated antigen (TAA), internalization of the complex through receptor-mediated endocytosis, and subsequent release of toxic regions that can lead to the death of target cells.[4,24] Therefore, the antitumor effect of ITs depends on several factors: the affinity of Abs for TAA expressed on the cell surface, the rate of internalization of the complex, and the inherent efficacy and specificity of the toxin.[25] Immunotoxin-based anti-PD-L1 mAb is considered to be an effective tumor treatment method in theory, because: (i) the immune checkpoint protein PD-L1 is broadly expressed in many cancers,[9,20,26,27] which is spectral in treatment; (ii) its expression is limited in tumor area but not in normal cells, the treatment is mainly aimed at tumor tissue, which makes PD-L1-specific treatment more accurate, and its side-effects limited; (iii) ELISA assay showed that PD-L1, as a transmembrane protein, was not released from the constitutively expressing PD-L1 cell membrane; and (iv) the key is that PD-L1 on tumor cells is glycosylated, so when anti-PD-L1 mAb is combined in the glycosylated domain, it will produce internalization,[28] which provides a good antitumor basis for IT-based treatment.[28,29] At present, PD-L1-specific treatment, such as PDL1-Dox[30] and PD-L1-AuNP-DOX[31] in the form of an Ab-drug conjugate, have shown some promising results. However, few studies focus on the generation of PD-L1 by ITs. To optimize the therapeutic effect and overcome immune checkpoint inhibitor resistance, we established a PD-L1-CUS IT, and verified its specific antitumor effect and its safety as an IT in the treatment of tumor.

D-CUS_{245C} showed potency in the picomolar range in the cytotoxicity assay, and the IC_{50} is approximately 100- to 1000-fold lower compared with other type I RIP-based conjugates, such as rituximab/saporin-S6. The IC_{50} values of rituximab/saporin-S6 for the $CD20^+$ cell lines, Raji and D430B, is 152 and 198 pmol/L, respectively.[32]

It is worth noting that MDA-MB-231 cells are most sensitive to D-CUS_{245C}, with an IC_{50} value of 0.14 pmol/L, 10^7 times lower than other PD-L1 Ab-based conjugates; eg the IC_{50} value of PDL1-Dox[30] in MDA-MB-231 cells is 1.25 μmol/L. According to a report, the response of TNBC patients to PD-1 inhibitors was relatively moderate (19%).[33] This means that new treatments or combination therapies are needed to improve the effect of TNBC. Accumulating evidence from multiple trials indicated that the combination of immune checkpoint inhibitors and other anticancer agents in TNBC has achieved more significant results than monotherapy.[34–36] Cheung et al[37] reported the use of V6A, a second-generation interleukin-2 receptor-targeted diphtheria fusion toxin, in conjunction with anti-PD-1 mAb as sequential immunotherapies eliciting a remarkable inhibition of tumor growth. Likewise, the immune response and survival rate induced by D2C7-IT can be effectively augmented and significantly improved by the combination of anti-CTLA-4/ anti-PD-1/anti-PD-L1 therapies in murine models of glioma.[38] D-CUS_{245C} has a potent cytotoxicity effect on MDA-MB-231 cells, suggesting that combined therapy with immune checkpoint inhibitors could be a promising anticancer therapeutic strategy for TNBC.

Results from ELISA showed that the sPD-L1 level in the culture supernatant of PD-L/SPC-A-1 cells was higher than that of MDA-MB-231 cells, and it was found that the inhibition rate of 0.8 mg/kg D-CUS_{245C} was 67% in PD-L1/SPC-A-1-derived xenografts, which means that the sPD-L1 level in peripheral blood did not neutralize the antitumor effect of the IT. The first-generation ITs were constructed using chemical coupling methods with an intact Ab. In this study, D-CUS_{245C} was constructed by a unique group of amine- and sulfhydryl-reactive heterobifunctional cross-linkers-SPDP. Although D-CUS_{245C} showed a clear inhibition of tumor growth in s.c. tumor-bearing xenograft models, poor penetration for D-CUS_{245C} into the tumor local region is the main obstacle to the treatment of solid tumors. The emergence of recombinant technologies has revolutionized the production of mAbs.[39] Currently, most of the ITs in clinical trials have been designed as recombinant fusion proteins linking to different Ab fragments, such as a flexible peptide, a disulfide bridge, or both, with reduced size and improved tumor penetration, to achieve greater specificity and antitumor efficacy.[4,40,41] Thus, in future experimental research, we hope to generate fusion ITs by genetic recombination technology to improve their tumor penetration and explore their antitumor activity, providing a theoretical basis to expand the PD-L1 monoclonal therapeutic window.

ACKNOWLEDGMENTS

We thanks Dr Liqun Luo for help with the experiment. This research was funded by the National Science Foundation of China (No. 30772587), the Natural Science Foundation of Fujian Province (No. 2016J01769), the Fujian Province health and family planning scientific research talent training project (No. 2018-CX-40), and

Startup Fund for scientific research, Fujian Medical University (No. 2019QH1196).

CONFLICT OF INTEREST

The authors have no conflict of interest.

ORCID

Caiyun Zhang http://orcid.org/0000-0002-8538-3180

REFERENCES

1. Kavousipour S, Khademi F, Zamani M, et al. Novel biotechnology approaches in colorectal cancer diagnosis and therapy. *Biotechnol Lett*. 2017;39(6):785-803.
2. Nasiri H, Valedkarimi Z, Aghebati-Maleki L, et al. Antibody-drug conjugates: promising and efficient tools for targeted cancer therapy. *J Cell Physiol*. 2018;233(9):6441-6457.
3. Allahyari H, Heidari S, Ghamgosha M, et al. Immunotoxin: a new tool for cancer therapy. *Tumour Biol*. 2017;39(2):1010428317692226.
4. Kreitman RJ. Recombinant immunotoxins containing truncated bacterial toxins for the treatment of hematologic malignancies. *BioDrugs*. 2009; 23(1):1–13.
5. Dougan M, Dranoff G. Immune therapy for cancer. *Annu Rev Immunol*. 2009;27(1):83–117.
6. Choudhary S, Mathew M, Verma RS. Therapeutic potential of anticancer immunotoxins. *Drug Discovery Today*. 2011;16(11–12):495-503.
7. Niesen J, Stein C, Brehm H, et al. Novel EGFR-specific immunotoxins based on panitumumab and cetuximab show in vitro and ex vivo activity against different tumor entities. *J Cancer Res Clin Oncol*. 2015;141(12):2079-2095.
8. Tomé-Amat J, Olombrada M, Ruiz-de-la-Herrán J, et al. Efficient in vivo antitumor effect of an immunotoxin based on ribotoxin α-sarcin in nude mice bearing human colorectal cancer xenografts. *SpringerPlus*. 2015;4:168.
9. Freeman GJ, Long AJ, Iwai Y, et al. Engagement of the PD-1 immunoinhibitory receptor by a novel B7 family member leads to negative regulation of lymphocyte activation. *J Exp Med*. 2000;192(7):1027-1034.
10. Li X, Shao C, Shi Y, et al. Lessons learned from the blockade of immune checkpoints in cancer immunotherapy. *J Hematol Oncol*. 2018;11(1):31.
11. John Wherry E. T cell exhaustion. *Nat Immunol*. 2011;12(6):492-499.
12. Pardoll DM. The blockade of immune checkpoints in cancer immunotherapy. *Nat Rev Cancer*. 2012;12(4):252-264.
13. Mahoney KM, Rennert PD, Freeman GJ. Combination cancer immunotherapy and new immunomodulatory targets. *Nat Rev Drug Discovery*. 2015;14(8):561-584.
14. Hou X, Meehan EJ, Xie J, et al. Atomic resolution structure of cucurmosin, a novel type 1 ribosome-inactivating protein from the sarcocarp of *Cucurbita moschata*. *J Struct Biol*. 2008;164(1):81-87.
15. Chen M, Ye X, Cai J, et al. Crystallization and preliminary crystallographic study of cucurmosin, a ribosome-inactivating protein from the sarcocarp of *Cucurbita moschata*. *Acta Crystallogr D Biol Crystallogr*. 2000;56(Pt 5):665-666.
16. Xiong J, Zhang C, Shuifa WU, et al. Recombinant cucurmosin-based immunotoxin targeting HER-2 with potent in vitro anti-cancer cytotoxicity. *Biochem Biophys Res Comm*. 2019;513(1):15-21.
17. Deng C, Xiong J, Xiaofan GU, et al. Novel recombinant immunotoxin of EGFR specific nanobody fused with cucurmosin, construction and antitumor efficiency in vitro. *Oncotarget*. 2017;8(24):38568-38580.
18. Syed YY. Durvalumab: first global approval. *Drugs*. 2017;77(12):1369-1376.
19. Gray JE, Villegas A, Daniel D, et al. Three-year overall survival with durvalumab after chemoradiotherapy in stage III NSCLC-update from PACIFIC. *J Thorac Oncol*. 2019;15(2):288-293.
20. Dong H, Strome SE, Salomao DR, et al. Tumor-associated B7–H1 promotes T-cell apoptosis: a potential mechanism of immune evasion. *Nat Med*. 2002;8(8):793-800.
21. O'Donnell JS, Long GV, Scolyer RA, et al. Resistance to PD1/PDL1 checkpoint inhibition. *Cancer Treat Rev*. 2017;52:71-81.
22. Zamboni M, Brigotti M, Rambelli F, et al. High-pressure-liquid-chromatographic and fluorimetric methods for the determination of adenine released from ribosomes by ricin and gelonin. *Biochem J*. 1989;259(3):639-643.
23. Endo Y, Mitsui K, Motizuki M, et al. The mechanism of action of ricin and related toxic lectins on eukaryotic ribosomes. The site and the characteristics of the modification in 28 S ribosomal RNA caused by the toxins. *J Biol Chem*. 1987;262(12):5908-5912.
24. Tomé-Amat J, Ruiz-de-la-Herrán J, Martínez-del-Pozo Á, et al. α-sarcin and RNase T1 based immunoconjugates: the role of intracellular trafficking in cytotoxic efficiency. *FEBS J*. 2015;282(4):673-684.
25. Hexham JM, Dudas D, Hugo R, et al. Influence of relative binding affinity on efficacy in a panel of anti-CD3 scFv immunotoxins. *Mol Immunol*. 2001;38(5):397-408.
26. Gatalica Z, Snyder C, Maney T, et al. Programmed cell death 1 (PD-1) and its ligand (PD-L1) in common cancers and their correlation with molecular cancer type. *Cancer Epidemiol Biomarkers Prev*. 2014;23(12):2965-2970.
27. Konishi J, Yamazaki K, Azuma M, et al. B7–H1 expression on non-small cell lung cancer cells and its relationship with tumor-infiltrating lymphocytes and their PD-1 expression. *Clin Cancer Res*. 2004;10(15):5094-5100.
28. Li CW, Lim SO, Chung EM, et al. Eradication of triple-negative breast cancer cells by targeting glycosylated PD-L1. *Cancer Cell*. 2018;33(2):187–201.e10.
29. Zhang Z, Wang Q, Liu Q, et al. Dual-Locking nanoparticles disrupt the PD-1/PD-L1 pathway for efficient cancer immunotherapy. *Adv Mater*. 2019;31(51):e1905751.
30. Sau S, Petrovici A, Alsaab HO, et al. PDL-1 antibody drug conjugate for selective chemo-guided immune modulation of cancer. *Cancers (Basel)*. 2019;11(2):232.
31. Emami F, Banstola A, Vatanara A, et al. Doxorubicin and anti-PD-L1 antibody conjugated gold nanoparticles for colorectal cancer photochemotherapy. *Mol Pharm*. 2019;16(3):1184-1199.
32. Bortolotti M, Bolognesi A, Battelli M, Polito L. High in vitro anti-tumor efficacy of dimeric rituximab/saporin-S6 immunotoxin. *Toxins (Basel)*. 2016;8(6):192.
33. Polk A, Svane IM, Andersson M, et al. Checkpoint inhibitors in breast cancer – current status. *Cancer Treat Rev*. 2018;63:122-134.
34. Adams S, Diamond JR, Hamilton E, et al. Atezolizumab plus nab-paclitaxel in the treatment of metastatic triple-negative breast cancer with 2-year survival follow-up: a phase 1b clinical trial. *JAMA Oncol*. 2019;5(3):334-342.
35. Liedtke C, Mazouni C, Hess KR, et al. Response to neoadjuvant therapy and long-term survival in patients with triple-negative breast cancer. *J Clin Oncol*. 2008;26(8):1275-1281.
36. Pennisi A, Kieber-Emmons T, Makhoul I, et al. Relevance of pathological complete response after neoadjuvant therapy for breast cancer. *Breast Cancer*. 2016;10:103-106.
37. Cheung LS, Fu J, Kumar P, et al. Second-generation IL-2 receptor-targeted diphtheria fusion toxin exhibits antitumor activity and synergy with anti-PD-1 in melanoma. *Proc Natl Acad Sci USA*. 2019;116(8):3100-3105.
38. Chandramohan V, Bao X, Yu X, et al. Improved efficacy against malignant brain tumors with EGFRwt/EGFRvIII targeting immunotoxin and checkpoint inhibitor combinations. *J Immunother Cancer*. 2019;7(1):142.

39. Lazaro-Gorines R, Ruiz-de-la-Herran J, Navarro R, et al. A novel carcinoembryonic antigen (CEA)-targeted trimeric immunotoxin shows significantly enhanced antitumor activity in human colorectal cancer xenografts. *Sci Rep*. 2019;9(1):11680.
40. Brinkmann U. Recombinant antibody fragments and immunotoxin fusions for cancer therapy. *In vivo (Athens, Greece)*. 2000;14(1):21-27.
41. Carreras-Sangrà N, Tomé-Amat J, García-Ortega L, et al. Production and characterization of a colon cancer-specific immunotoxin based on the fungal ribotoxin α-sarcin. *Protein Eng Des Sel*. 2012;25(8):425-435.

How to cite this article: Zhang C, Xiong J, Lan Y, et al. Novel cucurmosin-based immunotoxin targeting programmed cell death 1-ligand 1 with high potency against human tumor in vitro and in vivo. *Cancer Sci*. 2020;00:1–11. https://doi.org/10.1111/cas.14549